https://ntrs.nasa.gov/search.jsp?R=19800012795 2020-03-21T18:16:51+00:00Z

LOAN COPY: RETURN TO
AFWL TECHNICAL LIBRARY
KIRTLAND AFB, N.M.

NASA
TP
1627

NASA Technical Paper 1627

Comparison of Predicted and Experimental Real-Gas Pressure Distributions on Space Shuttle Orbiter Nose for Shuttle Entry Air Data System

Judy L. Shinn

APRIL 1980

NASA

TECH LIBRARY KAFB, NM
0134596

NASA Technical Paper 1627

Comparison of Predicted and Experimental Real-Gas Pressure Distributions on Space Shuttle Orbiter Nose for Shuttle Entry Air Data System

Judy L. Shinn
Langley Research Center
Hampton, Virginia

National Aeronautics
and Space Administration

**Scientific and Technical
Information Office**

1980

SUMMARY

An experimental investigation of inviscid real-gas effects on the pressure distribution along the Space Shuttle Orbiter nose center line up to an angle of attack of 32^{o} was performed in the Langley Expansion Tube in support of the Shuttle Entry Air Data System (SEADS), which is an instrumentation system for the Orbiter Experiment (OEX) Program. Free-stream velocities from 4.8 to 6.6 km/s were generated at hypersonic conditions with helium, air, and CO_2, resulting in normal-shock density ratios from 3.7 to 18.4. The experimental results for pressure distribution agreed closely with numerical results using the method of Moretti and Bleich (AIAA J., vol. 5, no. 9, 1967). Modified Newtonian theory deviates from both experiment and the numerical results as angle of attack increases or shock density ratio decreases. An evaluation of the use of modified Newtonian theory for predicting SEADS pressure distributions in actual flight conditions was made through comparison with numerical predictions.

INTRODUCTION

The Orbiter Experiment (OEX) Program has recently developed several instruments which take advantage of the unique opportunity provided by the Space Shuttle Orbiter to investigate regimes of flight and flight operation not previously available for research (refs. 1 and 2). One of these instruments, the Shuttle Entry Air Data System (SEADS), is required to provide an accurate knowledge of vehicle attitude relative to the free stream and free-stream environment at altitudes below 80 km through instrumentation of the orbiter's base-line nose cap (refs. 2 and 3). Some prior wind-tunnel tests (refs. 3 and 4) have been performed to verify the SEADS concept; however, these tests were obtained at essentially perfect-gas conditions.

As a blunt body enters an atmosphere at hypersonic speeds, the gas molecules that pass through the bow shock are excited to higher vibrational and chemical energy modes (commonly known as real-gas effects). This excitation increases the degrees of freedom of the gas in the shock layer and thus increases the shock density ratio. Several previous investigations (refs. 5 to 9) have shown that the pressure distribution, shock shape, and other aerodynamic characteristics of a blunt body are dependent on the shock density ratio. With a wide range of normal-shock density ratios expected to be encountered by the Shuttle, real-gas effects on SEADS measured pressure distributions cannot be neglected.

Previous studies have shown (refs. 5 to 9) that inviscid real-gas effects can be simulated in a substitute test-gas flow which provides the correct value of shock density ratio with or without dissociation. One of the hypersonic facilities that can provide a range of shock density ratios is the Langley Expansion Tube (ref. 9). With this facility, different test gases may be used

to generate a range of shock density ratios (approximately from 3.7 to 19). Recently, shock shapes on blunt bodies in several test gases simulating various shock density ratios were measured in this facility (refs. 8 and 9). The results show very good agreement with several ideal-gas shock-shape predictions using the correct value of shock density ratio.

The purpose of this report is to present the results of the Space Shuttle Orbiter nose-cap pressure distribution up to an angle of attack of 32°, obtained from the Langley Expansion Tube tests for a range of shock density ratios to support the SEADS development. The test gases used are He, air, and CO_2; these gases provided a velocity range from 4.8 to 6.6 km/s. The results are compared with modified Newtonian theory and numerical predictions based on an inviscid flow-field solution. The adequacy of modified Newtonian theory for predicting the Space Shuttle Orbiter nose-cap pressure distribution in actual flight conditions is assessed through comparison with numerical prediction.

SYMBOLS

h	altitude, km
M	Mach number
N_{Re}	Reynolds number per meter
p	pressure, kN/m^2
T	temperature, K
U	velocity, km/s
X,Y,Z	full-scale reference axes used in Space Shuttle Orbiter design
α	angle of attack, deg
γ	ratio of specific heats
γ_E	isentropic exponent
ε	normal-shock density ratio, ρ_{5s}/ρ_5
θ_n	local inclination of body-surface normal referenced to Space Shuttle Orbiter water line, deg
$\theta_{n,max}$	value of θ_n where maximum pressure occurs physically
ρ	density, kg/m^3

Subscripts:

calc	calculated
eff	effective
meas	measured
t	stagnation conditions
1	state of quiescent test gas in front of incident shock in intermediate section
2	state of test gas behind incident shock in intermediate section
3	driver gas following unsteady expansion
4	driver-gas conditions at time of primary-diaphragm rupture
5	state of test-gas flow or free-stream conditions
5s	static conditions behind bow shock of model positioned at test section
5t	stagnation conditions behind bow shock of model positioned at test section
10	state of quiescent acceleration gas in front of incident shock in acceleration section
20	state of acceleration gas behind incident shock in acceleration section

TEST CONDITIONS AND APPARATUS

Expansion Tube

The Langley Expansion Tube is an impulse facility capable of generating hypersonic-hypervelocity flows in arbitrary test gases. This facility, which is described in more detail in references 10 to 14, is principally a cylindrical tube 15 cm in diameter. This tube is divided by diaphragms (primary and secondary) into three sections. For the present tests, the driver, or farthest upstream section, was pressurized with hydrogen to a nominal pressure of 3.3 MN/m^2. A steel diaphragm (primary diaphragm) separated this driver section from the intermediate section. After evacuation of this intermediate section, a test gas was introduced to yield a quiescent pressure of 3.45 kN/m^2 for He and 0.69 kN/m^2 for air or CO_2. The section farthest downstream, denoted the acceleration section, was separated from the intermediate section by a thin, polyester film diaphragm (secondary diaphragm). The test gas was also used as

the acceleration gas for a given test, but at a lower quiescent pressure ($16\ N/m^2$ for He, $6.7\ N/m^2$ for air, and $3.2\ N/m^2$ for CO_2).

The operating sequence, which is shown schematically in figure 1, begins with the rupture of the steel (primary) diaphragm. This rupture creates a shock wave which propagates into the quiescent test gas and encounters and ruptures the secondary diaphragm. A secondary incident shock wave then propagates into the acceleration gas while an upstream expansion wave moves into the shock-heated test gas. In passing through this upstream expansion wave, the test gas undergoes an isentropic unsteady expansion resulting in an increase in flow velocity and free-stream Mach number (refs. 10, 11, 14, and 15). Test models are positioned at the exit of the acceleration section. Flow through this section exhausts into a dump tank; hence, models are tested in an open jet which has a test-core diameter of approximately 7.6 cm. A detailed description of the basic components and auxiliary equipment of the expansion tube is presented in reference 12.

Test-Flow Conditions

Because of the nonideal behavior that exists during operation of the expansion tube (refs. 11, 14, 16, 17, and 18), it was found that the test-section flow quantities, predicted from a simplified model for unsteady expansion based on prerun initial conditions, are not in good agreement with measured flow quantities. In order to provide a means for obtaining accurate test-section conditions, computational schemes for a real-gas mixture based on three flow quantities measured in the immediate vicinity of the test section were derived (ref. 19). These schemes eliminate an explicit dependence upon measured or calculated upstream flow properties and thereby substantially reduce the uncertainty in the predicted test-section flow conditions. Such computational schemes were used to determine test-flow conditions for the present study. Nominal measured values of pitot pressure, static wall pressure, and incident shock velocity obtained by the time-of-arrival method near the test section were used as inputs to the program of reference 19. The calculated results of flow conditions for each test gas are as follows:

Test gas	$p_{5'}$, kN/m^2	$\rho_{5'}$, kg/m^3	$T_{5'}$, K	$\gamma_{E,5}$	$U_{5'}$, km/s	M_5	$N_{Re,5'}$ per meter	ε	$\gamma_{E,5s}$	$p_{5t'}$, kN/m^2	$T_{5t'}$, K
He	0.96	0.00137	337	1.667	6.6	6.10	3.93×10^5	3.7	1.667	53.1	4531
Air	1.93	.00478	1406	1.309	5.1	7.02	4.73	10.8	1.145	120.7	5985
CO_2	1.31	.00452	1533	1.155	4.8	8.33	4.21	18.4	1.146	103.4	3761

For the investigation of inviscid real-gas effect on blunt bodies, a test-gas flow with dissociation, which provides the correct value of shock density ratio, may be used for simulation. To compare the experimental results with a numerical prediction in a perfect-gas mode, a constant value of specific heat ratio across the shock is required as input. For the helium test in the expansion tube, the ratio of specific heats is constant across the shock (that

is, γ_5 is equal to γ_{5s}); therefore, the condition for perfect-gas flow is satisfied. However, the dependence of γ on temperature for air and CO_2 test gases, caused by excitation, results in the equilibrium ratio of specific heats in the postshock region being somewhat less than the free-stream value. To satisfy the condition of constant γ across the shock, effective values of specific heat ratio and Mach number for air and CO_2 were used as inputs to the numerical method for perfect-gas flow. (As illustrated in refs. 8 and 9, measured shock shapes for a flat-faced cylinder model in air and CO_2 expansion-tube flow were in good agreement with perfect-gas predictions, provided that the correct normal-shock density ratio was accounted for by using an effective value of γ and M.) These effective values were determined from ideal-gas, normal-shock relations (ref. 20) and are as follows:

$$\gamma_{eff} = \frac{1 + \varepsilon\left(1 - \frac{2}{M_{eff}^2}\right)}{\varepsilon - 1} \tag{1}$$

and

$$\frac{p_{5t}}{p_5} = \left[\frac{(\gamma_{eff} + 1)M_{eff}^2}{2}\right]^{\frac{\gamma_{eff}}{\gamma_{eff}-1}} \left(\frac{\gamma_{eff} + 1}{2\gamma_{eff}M_{eff}^2 - \gamma_{eff} - 1}\right)^{\frac{1}{\gamma_{eff}-1}} \tag{2}$$

where p_{5t} and p_5 are measured quantities. The normal-shock density ratio ε was obtained from the thermochemical equilibrium program of reference 19. These effective values obtained for the corresponding test conditions as tabulated above are as follows:

Test gas	M_{eff}	γ_{eff}
He	6.1	1.667
Air	7.5	1.165
CO_2	8.5	1.100

Model and Instrumentation

The measured pressure distributions presented here for He, air, and CO_2 flow were obtained with a 0.025-scale stainless steel model of the Space Shuttle Orbiter forebody. A side view of the model at the symmetry plane is shown in full-scale reference axes X,Y,Z in figure 2(a), and in actual dimensions in figure 2(b). Cross-sectional views are presented in figure 2(c). The location of all seven pressure orifices on the model are listed in table I, for convenience, in full-scale reference axes X,Y,Z. Orifices 1 to 5, as indicated by Y = 0, are located at the symmetry line; orifices 6 and 7 are at

symmetric locations off the plane of symmetry to provide a validation for flow symmetry at 0^{o} angle of sideslip. Although the cross section of the model base is slightly larger than that of the expansion-tube test core, care was taken in placing the model sting to keep the sonic line and pressure orifices within the test core for each test gas and angle of attack.

Since the expansion tube is characterized by an extremely short test time (approximately 250 μs), pressure instrumentation having very fast response is required. Ultra-miniature, piezoresistive pressure transducers having a diameter of 0.23 cm and a length of 0.42 cm were mounted flush with the model surface. The transducers were manufactured with a 0.051-cm-thick protector screen placed 0.025 cm from the sensing surface, which had a layer of room-temperature-vulcanizing (RTV) silicone resin deposited to protect it from thermal and radiation effects. A constant supply of 10 volts was used to excite these pressure transducers, which had a built-in bridge circuit. The output signal from the transducer was connected through an amplifier to a transient waveform recorder which was interfaced to a programmable calculator. A typical time history of the pressure measured at the seven orifices on the model is shown in figure 3.

Calibration of the transducers through the amplifier and data acquisition system was performed before and after each test run. The results showed an uncertainty of ±2 percent in relative sensitivity among the transducers and an uncertainty in absolute value of ±5 percent. The larger uncertainty in absolute value was attributable to the difficulty of determining accurately the supply pressure used for calibration.

PREDICTION METHOD

The numerical method used to predict the pressure distribution around the Shuttle nose surface is similar to the one described in reference 21. This method is a time-dependent, finite-difference technique by which the three-dimensional inviscid flow field about blunt bodies (both axisymmetric and non-axisymmetric) can be computed. Steady-flow solutions are obtained by starting with an initial estimate of the shock shape and flow field and allowing computations to proceed until no changes with time are observed. The basic inputs needed for the perfect-gas computation mode are γ_{eff}, M_{eff}, and the blunt-body geometry. The details of the geometry system used to model the Shuttle forebody for numerical computation are described in reference 22.

SPACE SHUTTLE ORBITER FLIGHT CONDITIONS

In order to study the effects of high-temperature gas chemistry on the Space Shuttle Orbiter nose pressure distribution, some information regarding flight conditions during the course of Shuttle entry is required. For the possible candidate entry trajectory (TN 14414.1), vehicle speed and angle of attack as a function of altitude were obtained from Rockwell International. The pressure, density, and temperature of the atmosphere at a given altitude were found in reference 23. Pressure, density, and vehicle speed for the given altitude were used as inputs to the equilibrium program of reference 19 to

obtain the flow conditions across the normal shock. In figures 4(a), 4(b), and 4(c), free-stream Mach number M_5, angle of attack α, and normal-shock density ratio ε are shown as a function of altitude. The method described in the previous section was also used to obtain an effective ratio of specific heats γ_{eff}. The variation of γ_{eff} as a function of altitude is shown in figure 4(d).

RESULTS AND DISCUSSION

Expansion-Tube Test Results

In reference 4, a modified Newtonian distribution was used for the basis of an algorithm developed to determine angle of attack and stagnation pressure from SEADS pressure measurements. The surface pressure distribution along the symmetry line was presented as a function of the local inclination of the body-surface normal referenced to the water line of the Shuttle. In the present study, the same functional variable is used to present experimental results and theoretical predictions.

As indicated in the section "Model and Instrumentation," pressure orifices 1 to 5 were located on the symmetry line, and orifices 6 and 7 provided a validation for flow symmetry at 0° angle of sideslip. For all the tests performed in the expansion tube, the model was at 0° angle of sideslip, and measured pressures at orifices 6 and 7 were found to be essentially identical. The pressure distributions presented here were obtained from the measurements at the five orifices along the symmetry line. Since simultaneous measurement of stagnation pressure was not possible with a separate pitot-pressure probe (because of the limited test core) during each test run, the pressure distribution was normalized with an estimated stagnation value based on measured orifice pressure near the stagnation point and on Newtonian theory.

Normalized pressure distributions (as a function of the local inclination of the body-surface normal referenced to the Shuttle water line θ_n), obtained in air test flow, are shown by the symbols in figure 5 for $\alpha = 0^\circ$, 20°, and 32°. The solid lines indicate the numerical results obtained by using the method of reference 21. The broken lines were calculated from modified Newtonian theory, which is simply $p = p_t \cos^2 (\theta_n - \alpha)$ when the angle of attack α is taken into account. In figures 6 and 7, similar results obtained in He and CO_2 test flows are shown for $\alpha = 20^\circ$ and 32°. The experimental results for all three test gases agree more favorably with the numerical prediction than with modified Newtonian theory, which tends to overpredict pressure along the leeward side of maximum pressure (i.e., toward the upper surface) when the angle of attack increases. For $\alpha = 32^\circ$, the difference between the numerical results (or the data) and modified Newtonian distribution around orifice 2 ($\theta_n = 0^\circ$) is about 10 percent. When an uncertainty of ± 2 percent in relative sensitivity among the transducers is considered in combination with other sources of error, the difference between the numerical predictions and modified Newtonian theory is generally small. However, the agreement between numerical predictions and experimental results is consistently superior to that between modified Newtonian theory and experimental results.

It is well known that the validity of Newtonian theory is based on the assumption of infinite shock density ratio (which is equivalent to assuming that the ratio of specific heats approaches unity). Under this assumption, modified Newtonian theory $\left(\cos^2 (\theta_n - \alpha)\right)$ predicts that the physical location for maximum pressure $\theta_{n,max}$ is at the geometrical location for maximum pressure; i.e., $\theta_{n,max} = \alpha$. Since the effective ratios of specific heats for air and CO_2 test flow are fairly close to 1 ($\gamma_{eff} = 1.165$ for air and $\gamma_{eff} = 1.100$ for CO_2), the difference between the value of $\theta_{n,max}$ determined by the numerical results (which agree with the experimental data) and the value of α is only 1.5^o for $\alpha = 32^o$ and less than 1^o for $\alpha = 20^o$ (shown in figs. 5 and 7). However, the effective ratio of specific heats for He test flow is much larger than 1. Consequently, the numerical results together with the experimental data in figure 6 show a larger displacement of $\theta_{n,max}$ from the geometrical stagnation point toward the windward side; i.e., $\theta_{n,max} - \alpha$ is approximately 4.5^o at $\alpha = 32^o$ and less than 2^o at $\alpha = 20^o$. For all three test gases, the displacement of $\theta_{n,max}$ appears to increase as angle of attack increases.

To further substantiate the effect of increasing γ_{eff} or α on the displacement of physical location for maximum pressure $\theta_{n,max}$ beyond present test results, a comparison of the wind-tunnel test results presented in reference 4 is made. The experimental results used for the analysis of reference 4 were obtained from the Langley Continuous-Flow Hypersonic Tunnel (Mach 10) which provides a nearly perfect air test flow having a value of γ_{eff} approximately equal to 1.4. Figure 8 is taken from reference 4 and shows a correlation for measured angle of attack α_{meas} with calculated angle of attack α_{calc} at 0^o sideslip for angles of attack up to 42^o. The result shows that α_{calc} is becoming increasingly larger than α_{meas} as the value of α increases. The calculated angle of attack was obtained by applying an algorithm based on a pressure distribution of $\cos^{2n} (\theta_n - \alpha_{calc})$ with $n \approx 1$ to the experimental results and thus represents the (experimentally determined) physical location for maximum pressure $\theta_{n,max}$. As shown in figure 8, the results obtained from the Continuous-Flow Hypersonic Tunnel data are consistent with the expansion-tube results in that the displacement $(\theta_{n,max} - \alpha)$ increases as α increases. Furthermore, a difference of 2.5^o between calculated and measured α at $\alpha = 32^o$, as estimated from figure 8 for $\gamma_{eff} \approx 1.4$, is compatible with the expansion-tube results: $\theta_{n,max} - \alpha$ is approximately 4.5^o for $\gamma_{eff} = 1.667$ and 1.5^o for $\gamma_{eff} = 1.165$.

In figures 9 and 10, comparison of normalized pressure distributions at the same angle of attack is made for the three test flows. The symbols represent the data; the lines indicate the numerical results of reference 21. For angles of attack of both 20^o and 32^o, the pressure distributions increase significantly on the windward side of maximum pressure but change only slightly on the leeward side when the effective ratio of specific heats γ_{eff} increases from 1.100 through 1.165 to 1.667.

Numerical Results for Space Shuttle Orbiter Flight Conditions

As mentioned in the section "Expansion-Tube Test Results," the expansion-tube test results were in good agreement with the numerical prediction of

reference 21 for several values of angle of attack α and effective ratios of specific heats γ_{eff}. Although simulation at exact values of α and γ_{eff} for the Shuttle Orbiter flight conditions presented in figures 4(b) and 4(d) was not obtained experimentally, the test results have verified that the numerical method of reference 21 accurately predicts the pressure distribution for the flight range of angle of attack and γ_{eff}. In figure 11, normalized pressure distributions, as a function of the local inclination of the body-surface normal referenced to the free-stream flow direction $\theta_n - \alpha$, are shown by broken lines for flight conditions at altitudes of 67.06, 60.96, 48.77, and 36.58 km. The input conditions used for the numerical computation (ref. 21) were obtained from figures 4(a), 4(b), and 4(d). The modified Newtonian distribution (solid line) is also shown in figure 11 for comparison. For all four orbiter flight conditions considered in figure 11, the angle of attack is 22° or greater, and as previously noted, modified Newtonian theory shows overprediction along the leeward side of maximum pressure. This result agrees with the results of expansion-tube tests at higher angles of attack.

The displacement of physical location for maximum pressure from the geometrical location $\theta_{n,max} - \alpha$ was also found to increase as γ_{eff} or α increased. For the input conditions used in obtaining numerical results in figure 11, a larger value of γ_{eff} is coupled with a smaller value of α and vice versa. This combination results in an overall small displacement $\theta_{n,max} - \alpha$, as indicated in figure 11. For the four cases considered, the displacement is not greater than 2.5°.

CONCLUDING REMARKS

An experimental investigation of inviscid real-gas effects on the Space Shuttle Orbiter nose pressure distribution up to an angle of attack of 32° was performed in the Langley Expansion Tube. Helium, air, and CO_2 were used as test gases to provide various effective ratios of specific heats of 1.667, 1.165, and 1.100, respectively. The results were compared with modified Newtonian theory and with a numerical prediction based on the inviscid flow-field solution of Moretti and Bleich (AIAA J., vol. 5, no. 9, 1967).

Normalized pressure distributions as a function of the local inclination of the body-surface normal referenced to the Shuttle water line, obtained in all three test gases, showed consistently better agreement with the numerical results when effective ratios of specific heats for real gases were used as inputs than with modified Newtonian theory. As the angle of attack increased, the difference between these two predictions became larger. At an angle of attack of 32°, modified Newtonian theory showed an overprediction on the leeward side of maximum pressure by as much as 10 percent, in comparison with the experimental data and numerical results.

As the angle of attack or effective ratio of specific heats increased, the physical location for maximum pressure determined by the numerical results and experimental data was found to shift away from the geometrical stagnation point toward the windward side. For the highest angle of attack and effective ratio of specific heats tested, the displacement was approximately 4.5°. This

increasing trend for displacement caused by increasing angle of attack and increasing effective ratio of specific heats was found to be consistent with the result concluded from Langley Continuous-Flow Hypersonic Tunnel tests where the effective ratio of specific heats was approximately 1.4.

To assess the adequacy of modified Newtonian theory for predicting Space Shuttle Orbiter nose pressure distributions in actual flight conditions through Shuttle Entry Air Data System (SEADS) measurement, comparisons were made with numerical predictions for the conditions at altitudes of 67.06, 60.96, 48.77, and 36.58 km. The results showed that modified Newtonian theory overpredicted the pressure along the leeward side of maximum pressure as a result of rather high angle of attack for all four conditions. Furthermore, because mixed combinations of larger or smaller values of angle of attack with smaller or larger values of effective ratio of specific heats existed for all the input conditions, the displacement of physical location for maximum pressure from the geometrical location was not more than 2.5°.

Langley Research Center
National Aeronautics and Space Administration
Hampton, VA 23665
February 27, 1980

REFERENCES

1. Langley Research Center OEX Task Team Report. NASA TM-80042, 1979.

2. Siemers, Paul M., III; and Larson, Terry J.: The Space Shuttle Orbiter and Aerodynamic Testing. AIAA Paper 78-790, Apr. 1978.

3. Siemers, Paul M., III: Shuttle Entry Air Data System. NASA paper presented at 1978 Air Data Systems Conference (Colorado Springs, Colorado), May 1978.

4. Wolf, H.; and Eades, J. B., Jr.: Analysis of the Shuttle Air Data System. NASA CR-145279, 1977.

5. Jones, Robert A.; and Hunt, James L. (With appendix A by James L. Hunt, Kathryn A. Smith, and Robert B. Reynolds, and appendix B by James L. Hunt and Lillian R. Boney): Use of Tetrafluoromethane To Simulate Real-Gas Effects on the Hypersonic Aerodynamics of Blunt Vehicles. NASA TR R-312, 1969.

6. Jones, Robert A.; and Hunt, James L.: Measured Pressure Distributions on Large-Angle Cones in Hypersonic Flows of Tetrafluoromethane, Air, and Helium. NASA TN D-7429, 1973.

7. Hunt, James L.; Jones, Robert A.; and Smith, Kathryn A.: Use of Hexafluoroethane To Simulate the Inviscid Real-Gas Effects on Blunt Entry Vehicles. NASA TN D-7701, 1974.

8. Miller, Charles G., III: A Comparison of Measured and Predicted Sphere Shock Shapes in Hypersonic Flows With Density Ratios From 4 to 19. NASA TN D-8076, 1975.

9. Miller, Charles G., III: Shock Shapes on Blunt Bodies in Hypersonic-Hypervelocity Helium, Air, and CO_2 Flows, and Calibration Results in Langley 6-Inch Expansion Tube. NASA TN D-7800, 1975.

10. Trimpi, Robert L.: A Preliminary Theoretical Study of the Expansion Tube, A New Device for Producing High-Enthalpy Short-Duration Hypersonic Gas Flows. NASA TR R-133, 1962.

11. Jones, Jim J.; and Moore, John A.: Exploratory Study of Performance of the Langley Pilot Model Expansion Tube With a Hydrogen Driver. NASA TN D-3421, 1966.

12. Moore, John A.: Description and Initial Operating Performance of the Langley 6-Inch Expansion Tube Using Heated Helium Driver Gas. NASA TM X-3240, 1975.

13. Miller, Charles G., III; and Jones, Jim J.: Incident Shock-Wave Characteristics in Air, Argon, Carbon Dioxide, and Helium in a Shock Tube With Unheated Helium Driver. NASA TN D-8099, 1975.

14. Shinn, Judy L.; and Miller, Charles G., III: Experimental Perfect-Gas Study of Expansion-Tube Flow Characteristics. NASA TP-1317, 1978.

15. Miller, Charles G., III: A Program for Calculating Expansion-Tube Flow Quantities for Real-Gas Mixtures and Comparison With Experimental Results. NASA TN D-6830, 1972.

16. Haggard, Kenneth V.: Free-Stream Temperature, Density, and Pressure Measurements in an Expansion Tube Flow. NASA TN D-7273, 1973.

17. Haggard, Kenneth V.; and Goad, William K.: A Comparison of Measured and Predicted Test Flow in an Expansion Tube With Air and Oxygen Test Gases. NASA TN D-8068, 1975.

18. Friesen, Wilfred J.: Use of Photoionization in Measuring Velocity Profile of Free-Stream Flow in Langley Pilot Model Expansion Tube. NASA TN D-4936, 1968.

19. Miller, Charles G., III: Computer Program of Data Reduction Procedures for Facilities Using CO_2-N_2-O_2-Ar Equilibrium Real-Gas Mixtures. NASA TM X-2512, 1972.

20. Ames Research Staff: Equations, Tables, and Charts for Compressible Flow. NACA Rep. 1135, 1953. (Supersedes NACA TN 1428.)

21. Moretti, Gino; and Bleich, Gary: Three-Dimensional Flow Around Blunt Bodies. AIAA J., vol. 5, no. 9, Sept. 1967, pp. 1557-1562.

22. Marconi, Frank; and Yaeger, Larry: Development of a Computer Code for Calculating the Steady Super/Hypersonic Inviscid Flow Around Real Configurations. Volume II - Code Description. NASA CR-2676, 1976.

23. U.S. Standard Atmosphere, 1976. NOAA, NASA, and U.S. Air Force, Oct. 1976.

TABLE I.- LOCATION OF PRESSURE ORIFICES IN FULL-SCALE

REFERENCE AXES X,Y,Z

Orifice	X		Y		Z	
	cm	in.	cm	in.	cm	in.
1	604.926	238.160	0	0	883.232	347.729
2	596.900	235.000	0	0	859.790	338.500
3	604.573	238.021	0	0	836.427	329.302
4	618.404	243.466	0	0	816.397	321.416
5	635.508	250.200	0	0	799.084	314.600
6	610.784	240.466	-34.290	-13.500	849.432	334.422
7	610.784	240.466	34.290	13.500	849.432	334.422

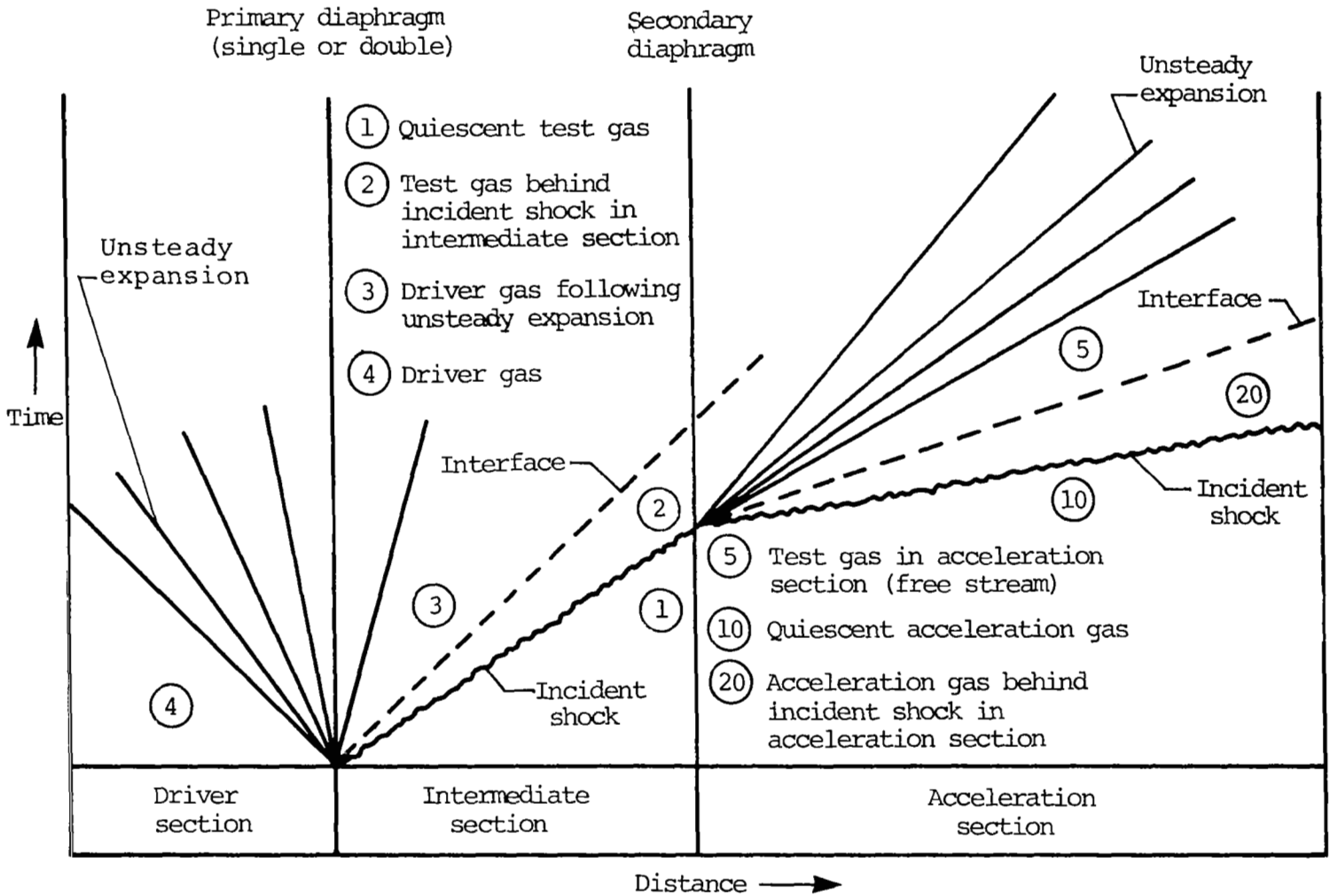

Figure 1.- Schematic diagram of expansion-tube flow sequence.

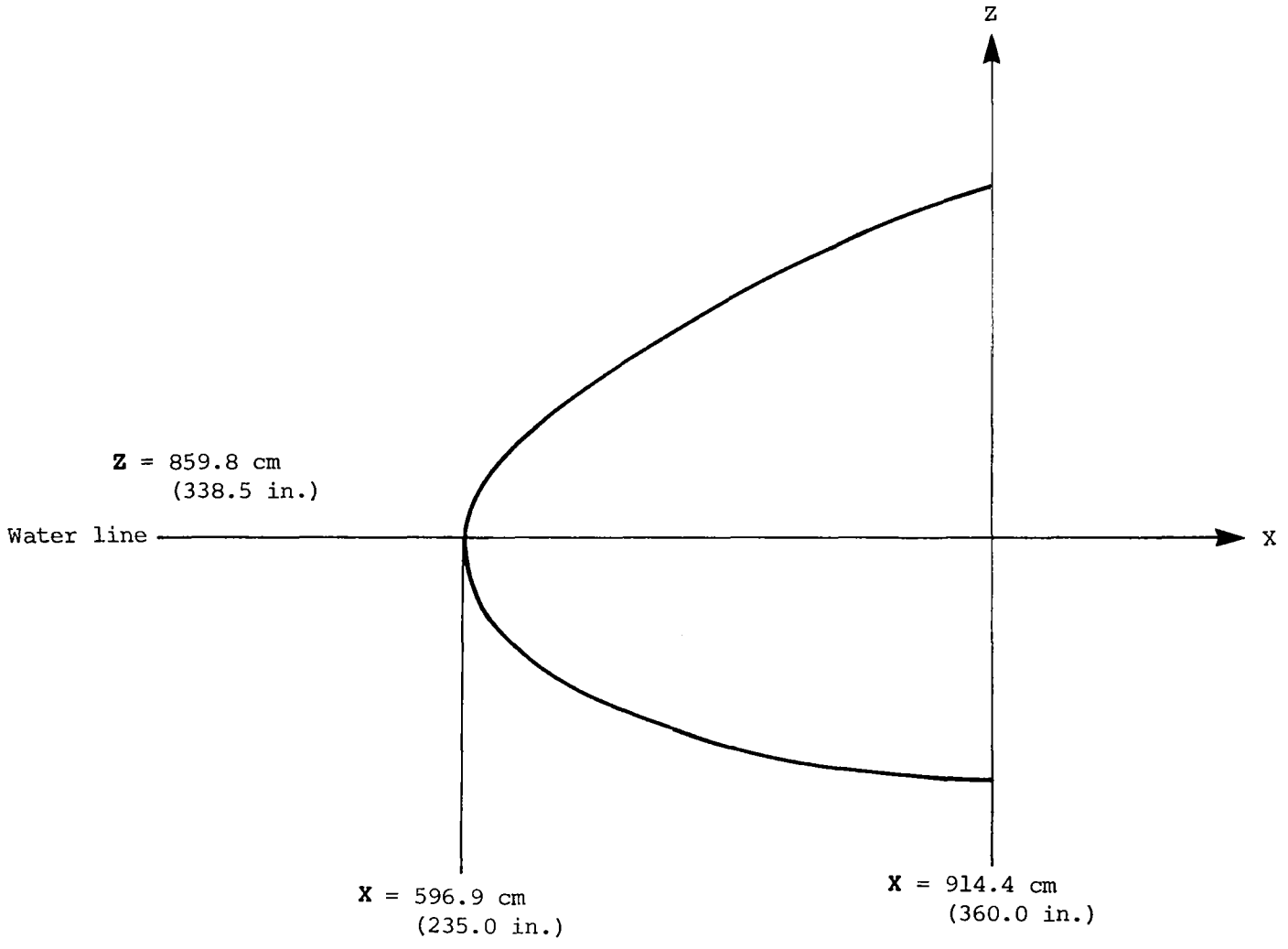

(a) Side view in full-scale reference axes. Y = 0.

Figure 2.- Space Shuttle Orbiter forebody model of 0.025 scale (X,Y,Z are full-scale reference axes).

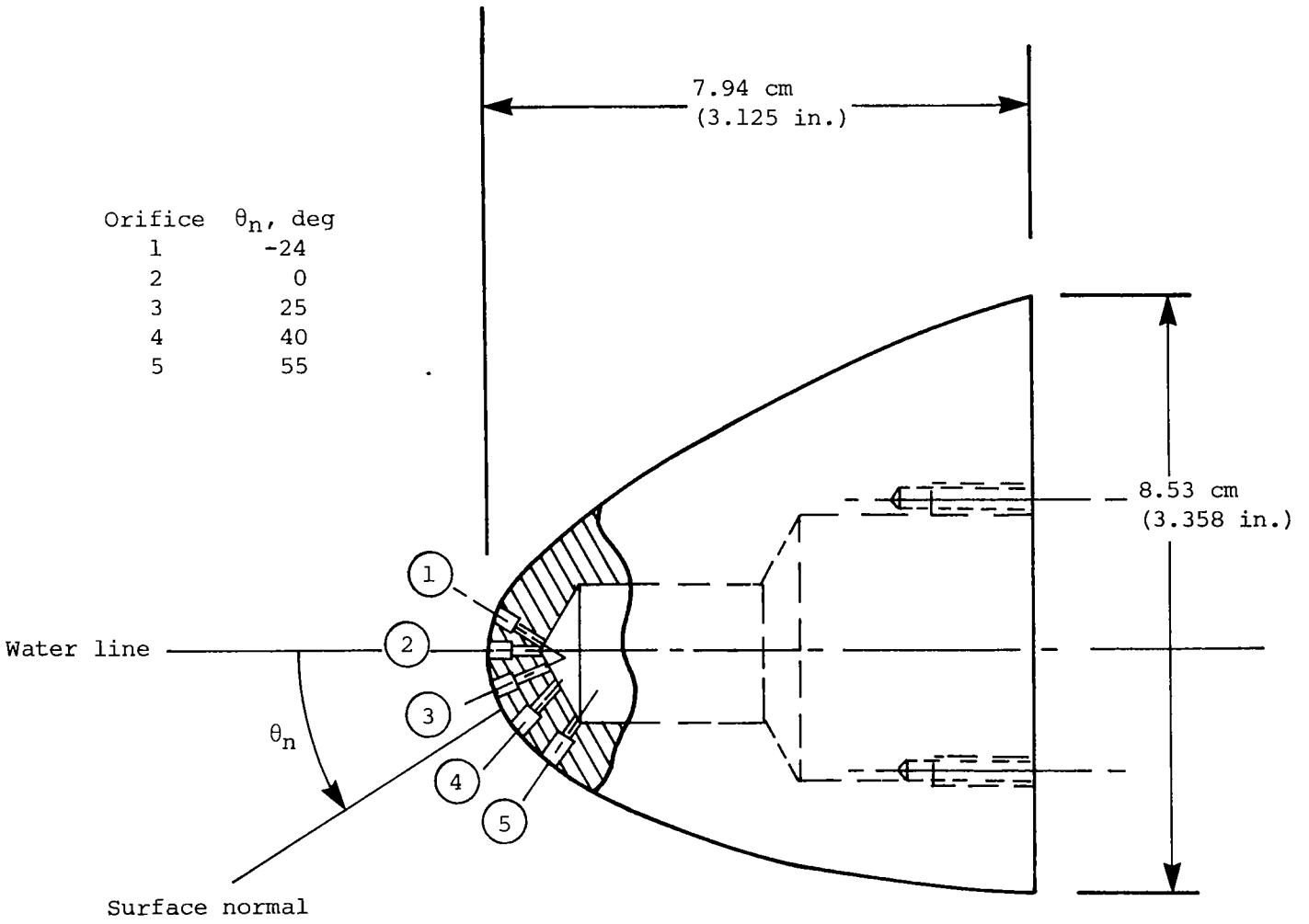

(b) Side view in actual dimensions. Y = 0.

Figure 2.- Continued.

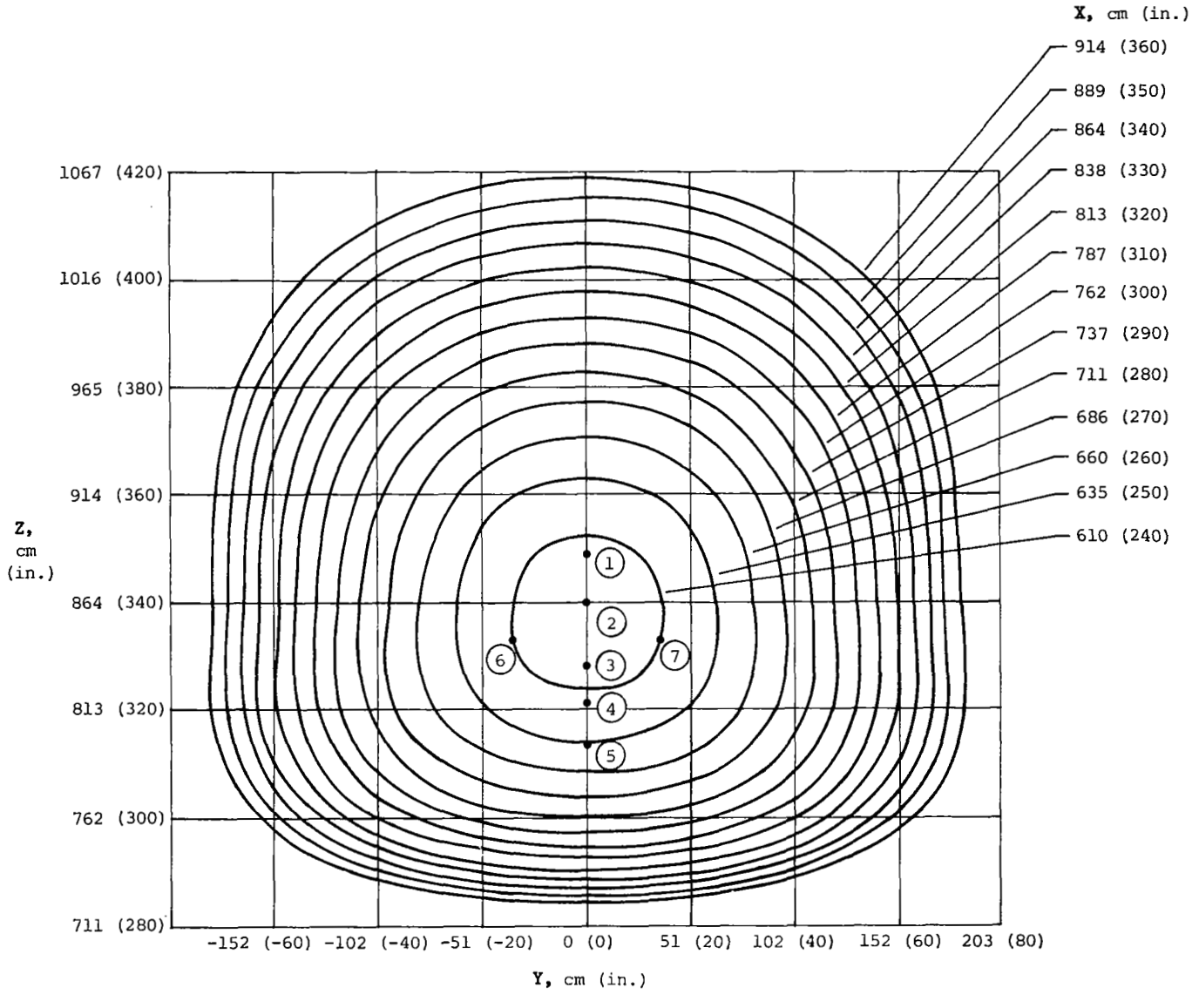

(c) Cross-sectional views at several values of X.

Figure 2.- Concluded.

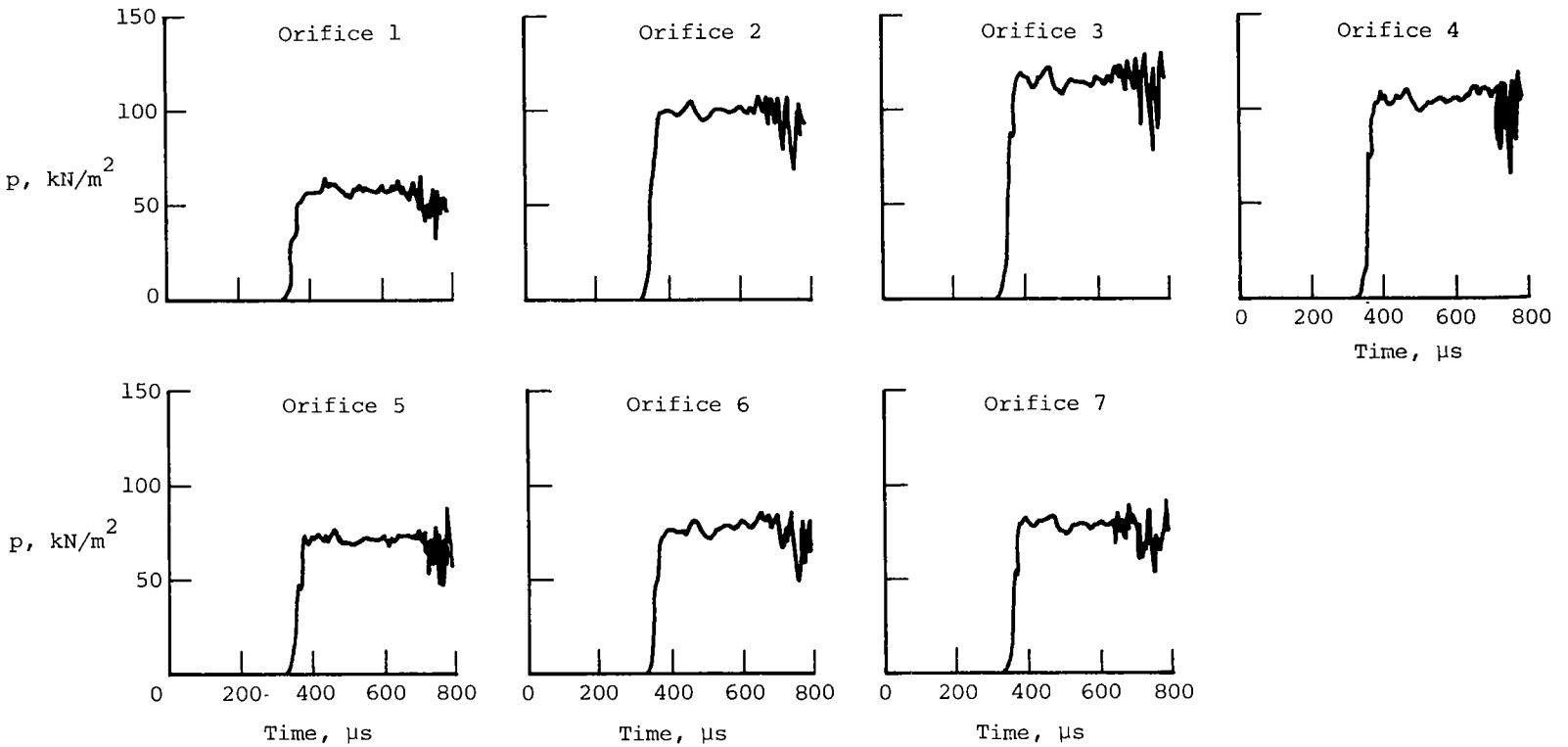

Figure 3.- Typical pressure time history measured at the seven orifices on Space Shuttle Orbiter nose model. Test gas, air; $\alpha = 20^{\circ}$.

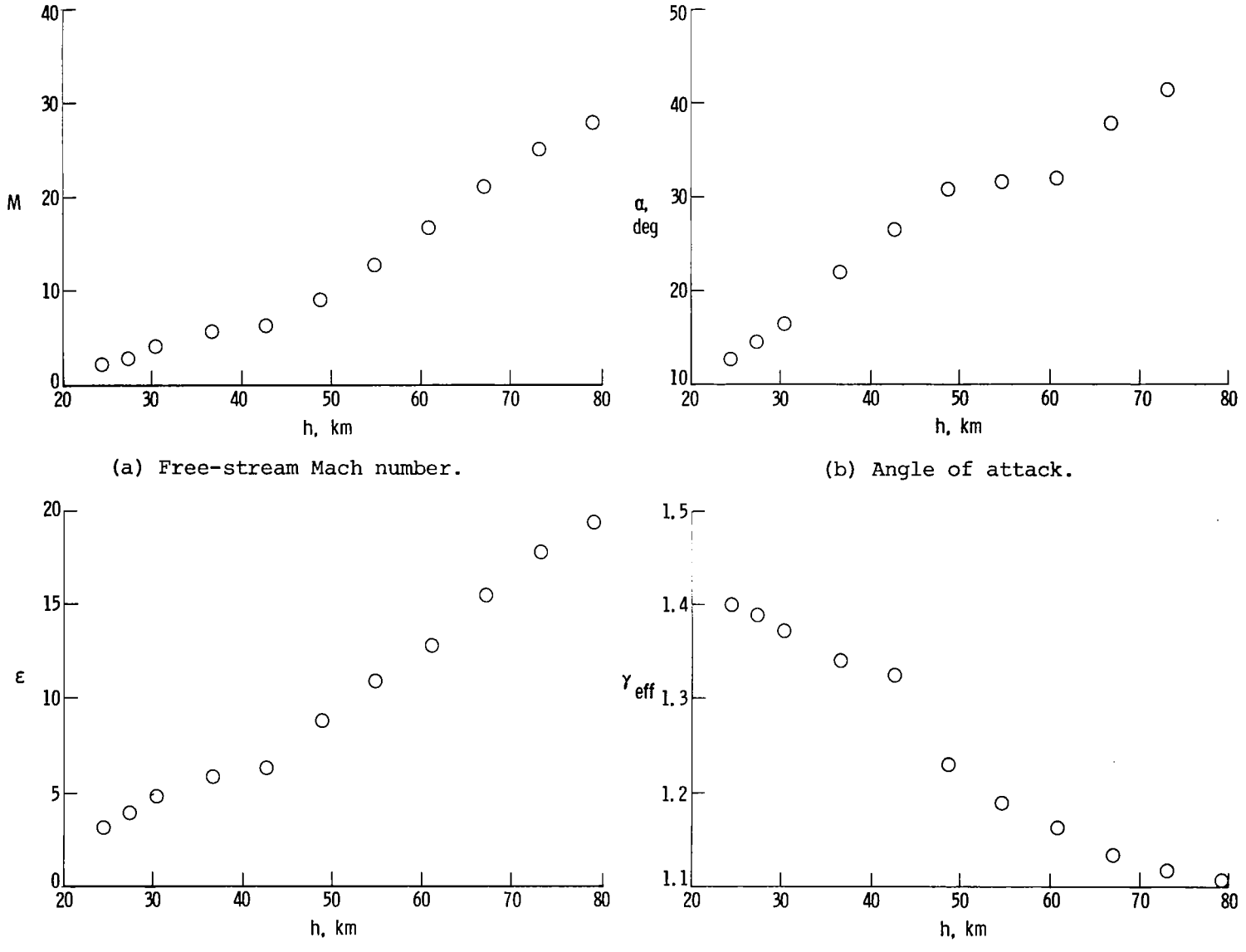

(a) Free-stream Mach number.

(b) Angle of attack.

(c) Normal-shock density ratio.

(d) Effective ratio of specific heats.

Figure 4.- Variation of free-stream Mach number, angle of attack, normal-shock density ratio, and effective ratio of specific heats with altitude for Space Shuttle trajectory TN 14414.1.

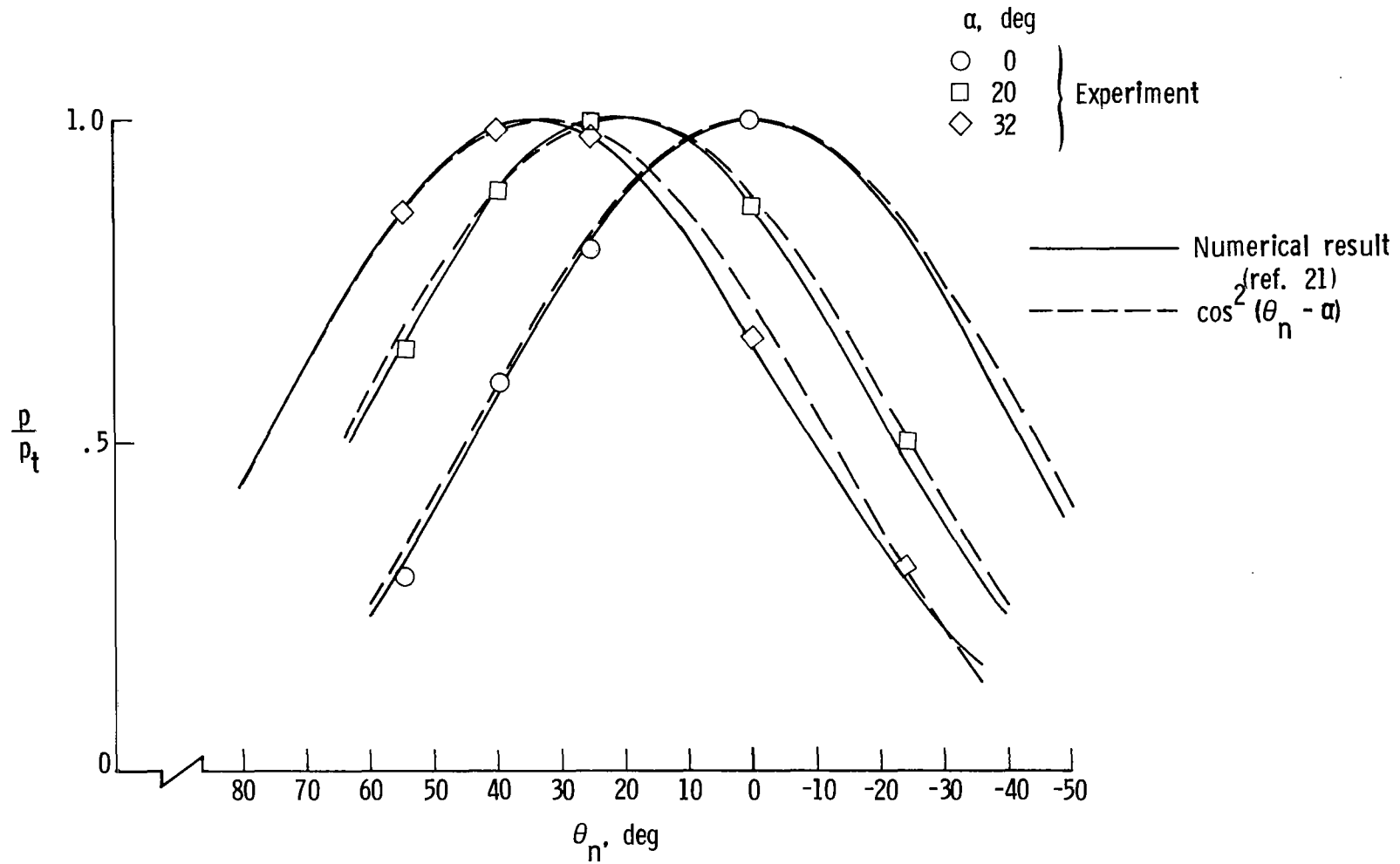

Figure 5.- Effect of α on normalized pressure distributions for air. $\gamma_{eff} = 1.165$; $M_{eff} = 7.5$.

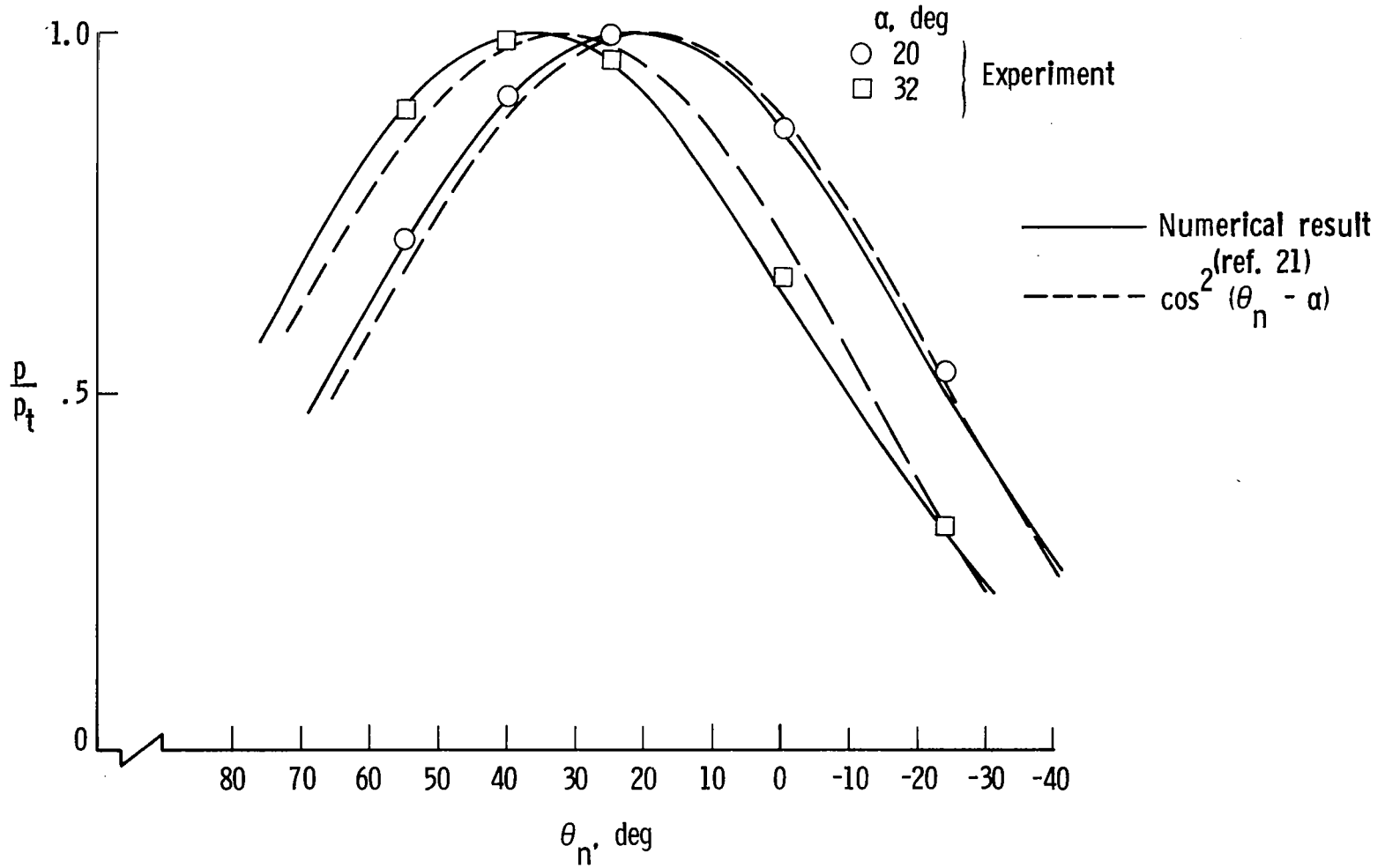

Figure 6.- Effect of α on normalized pressure distributions for He. $\gamma_{eff} = 1.667$; $M_{eff} = 6.1$.

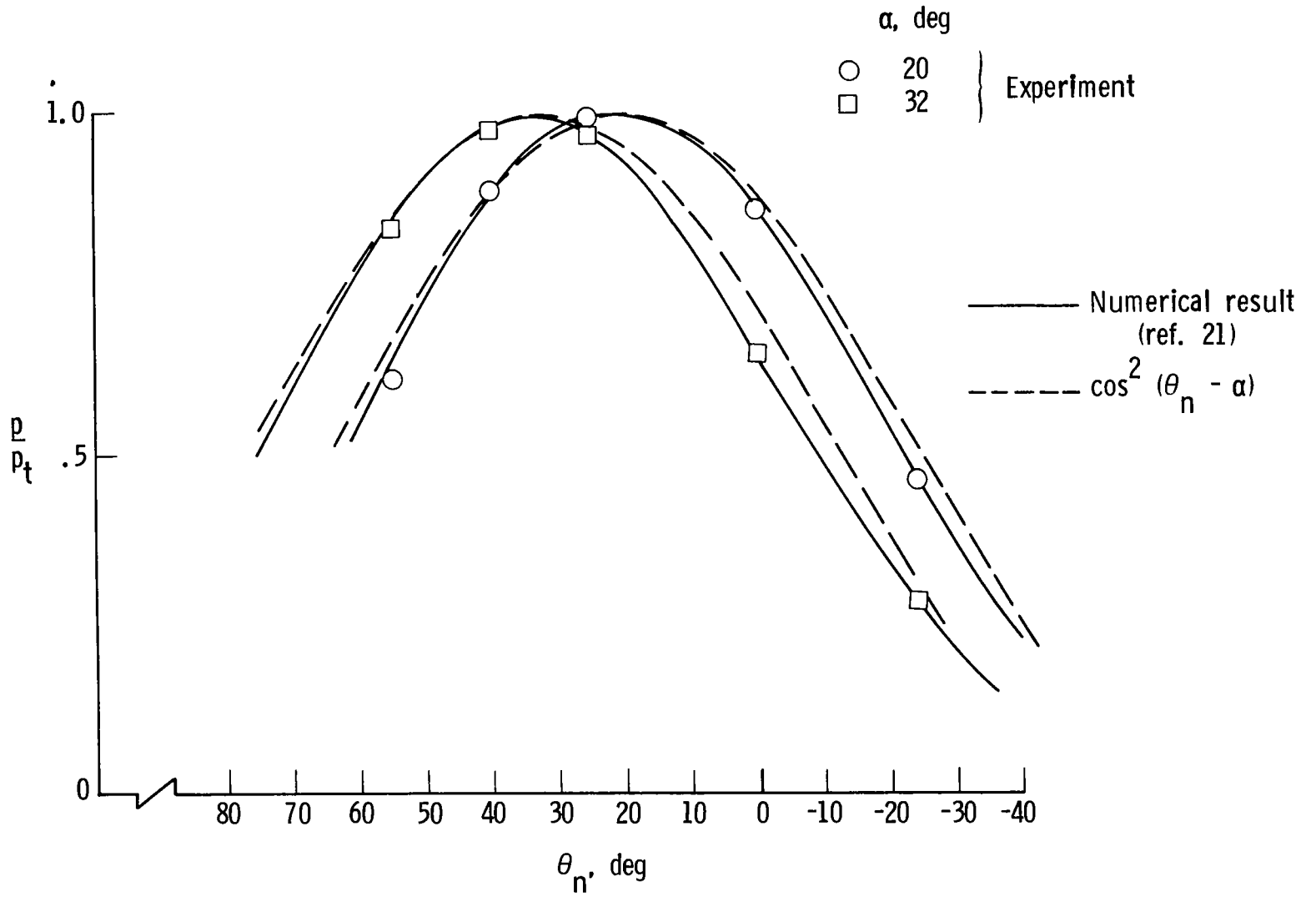

Figure 7.- Effect of α on normalized pressure distributions for CO_2. $\gamma_{eff} = 1.100$; $M_{eff} = 8.5$.

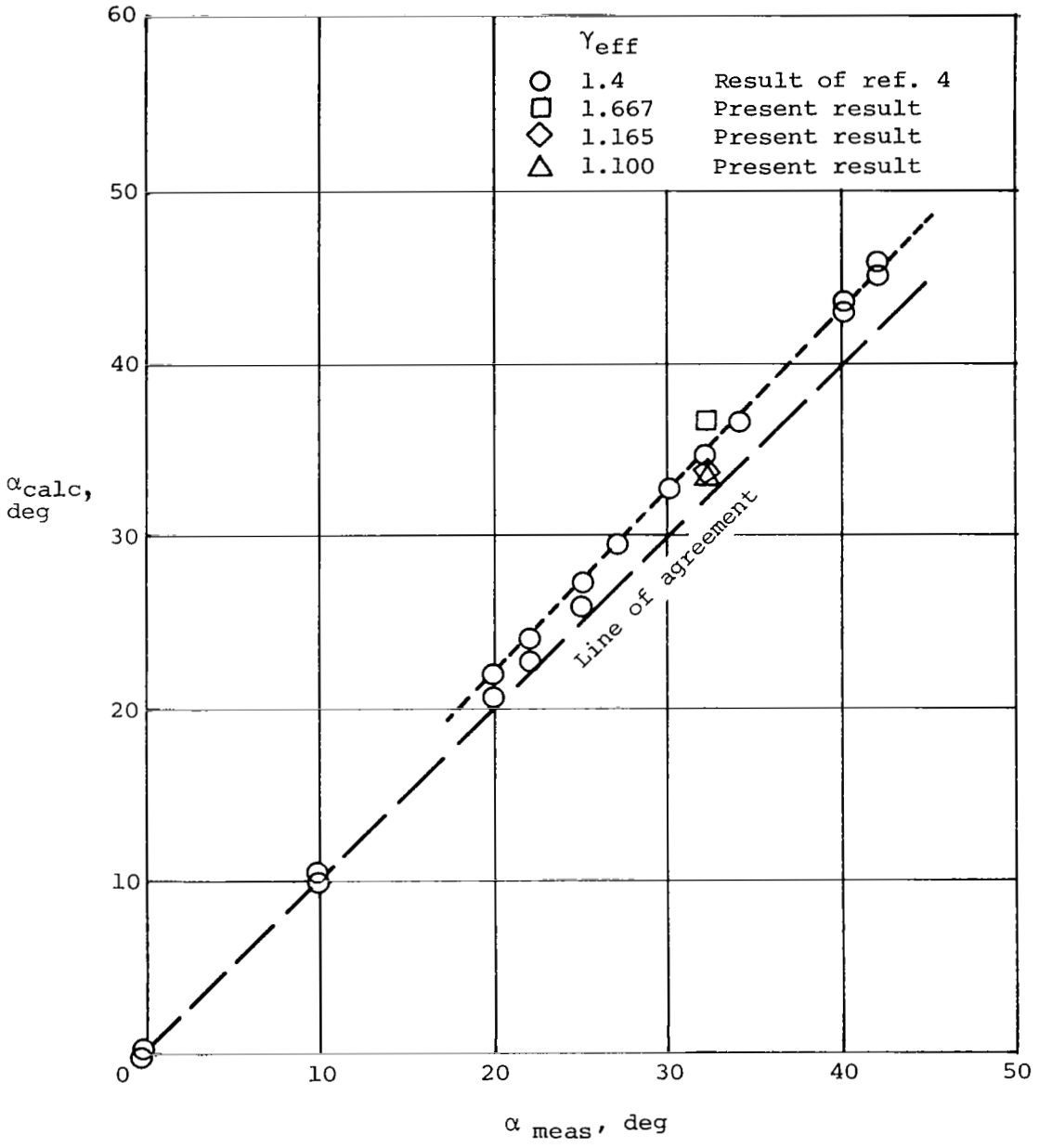

Figure 8.- Correlation for α_{meas} with α_{calc} at 0^{o} sideslip for Langley Continuous-Flow Hypersonic Tunnel tests; comparison is made with present results at $\alpha = 32^{o}$. (Obtained from fig. 1 of part VII, ref. 4.)

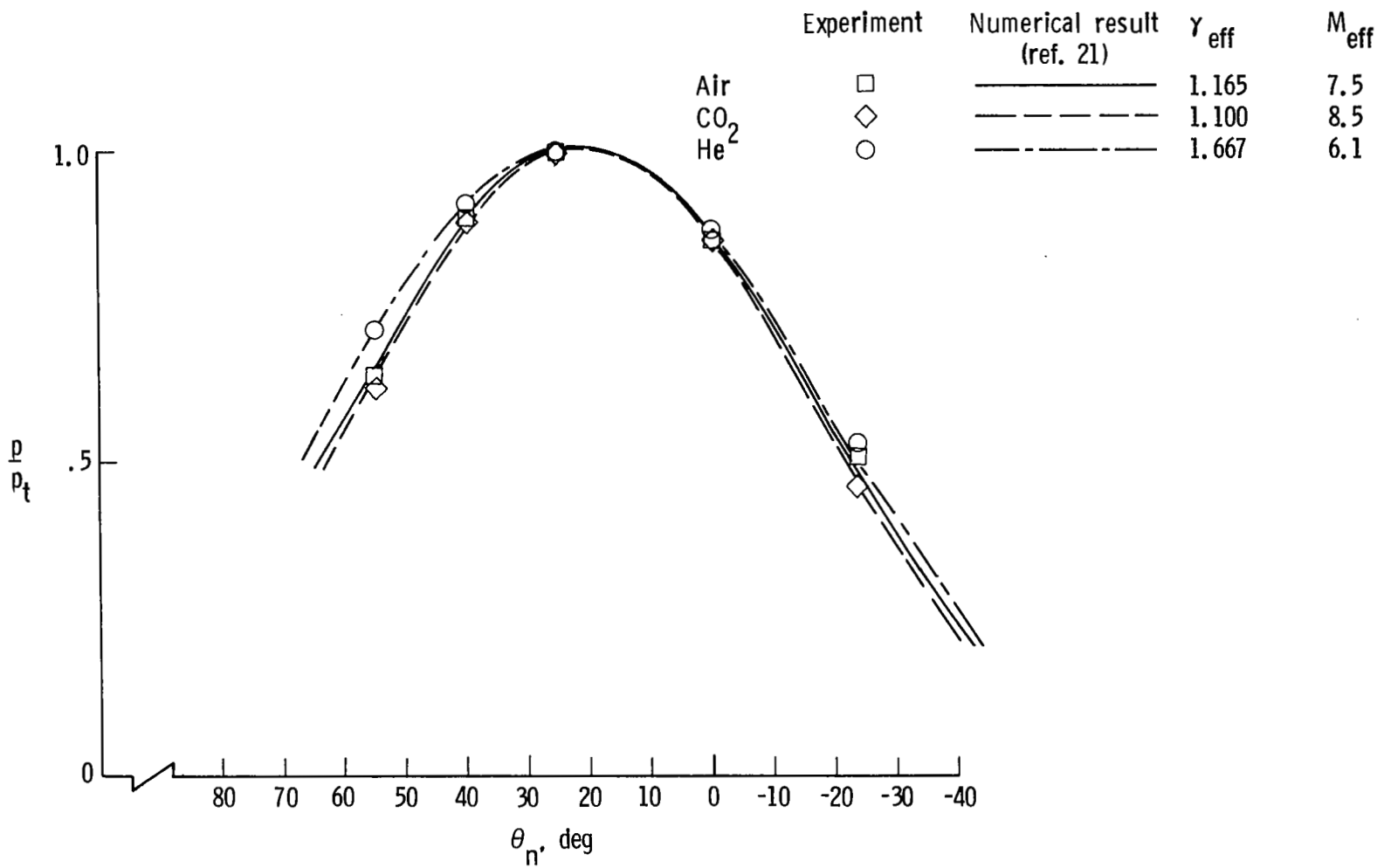

Figure 9.- Effect of γ_{eff} on normalized pressure distributions at $\alpha = 20^{\circ}$.

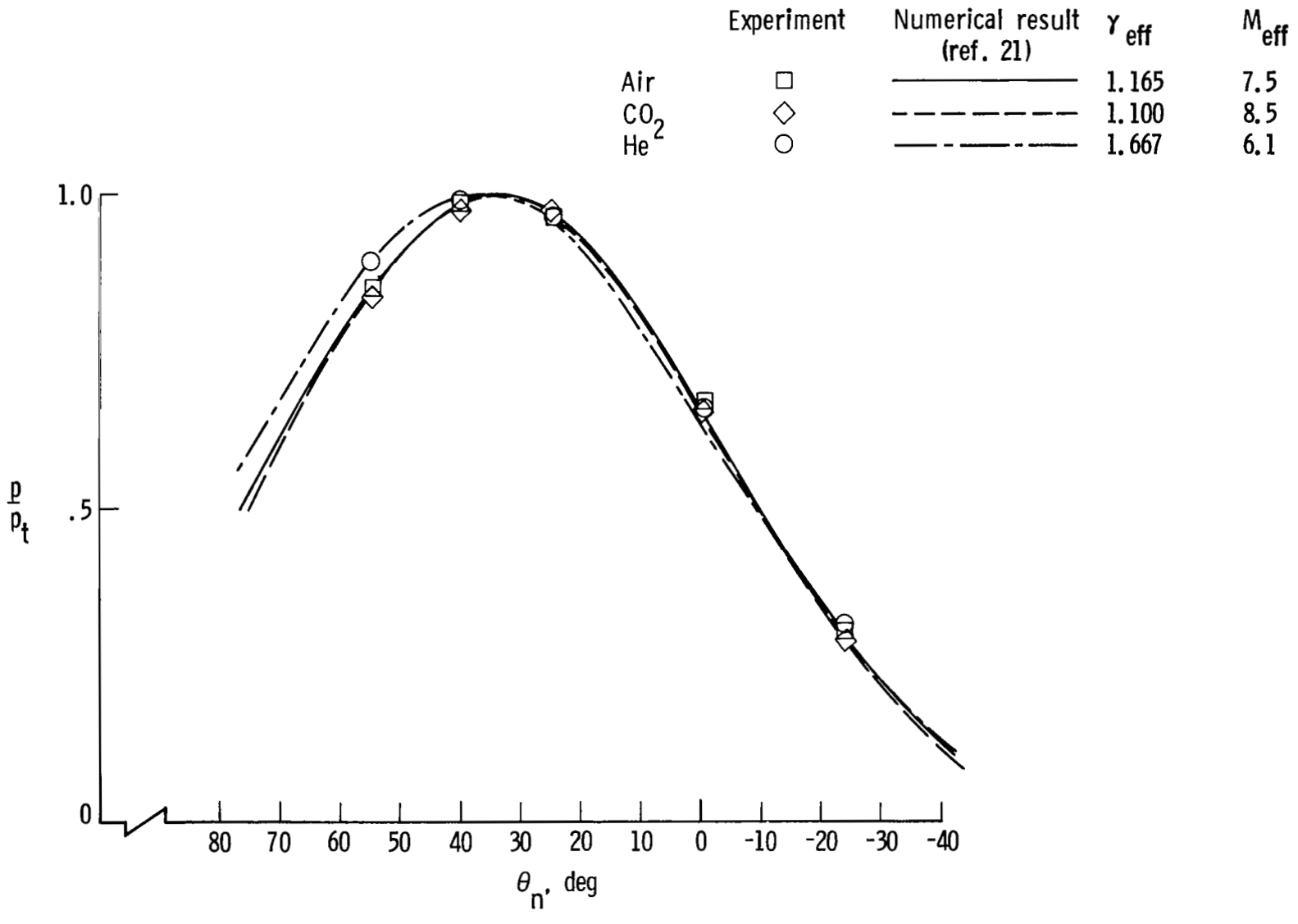

Figure 10.- Effect of γ_{eff} on normalized pressure distributions at $\alpha = 32^{o}$.

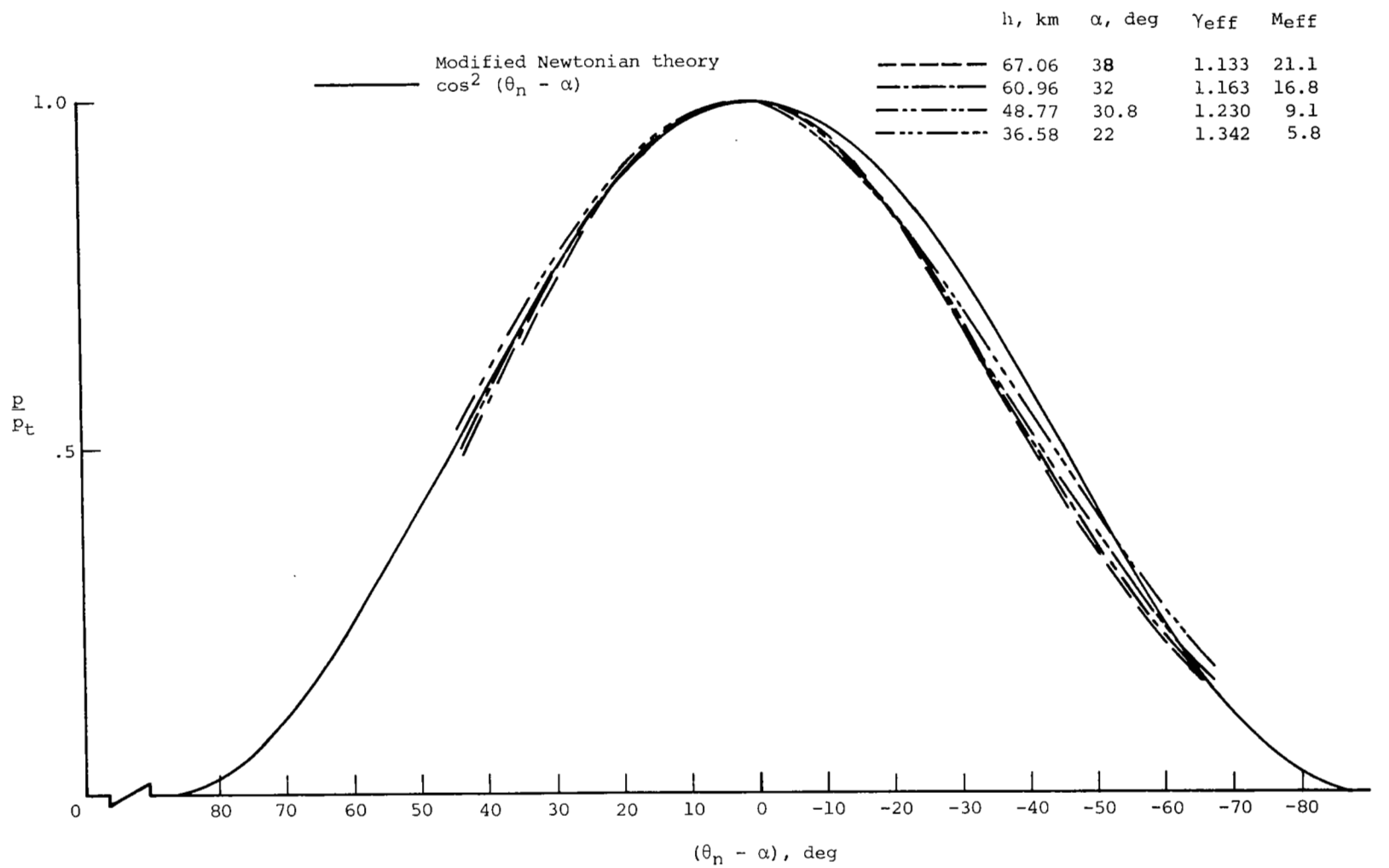

Figure 11.- Comparison of normalized pressure distributions obtained by using numerical method of reference 21 with modified Newtonian distribution for flight conditions.

1. Report No.	2. Government Accession No.	3. Recipient's Catalog No.
NASA TP-1627		

4. Title and Subtitle	5. Report Date
COMPARISON OF PREDICTED AND EXPERIMENTAL REAL-GAS PRESSURE DISTRIBUTIONS ON SPACE SHUTTLE ORBITER NOSE FOR SHUTTLE ENTRY AIR DATA SYSTEM	April 1980
	6. Performing Organization Code
7. Author(s)	8. Performing Organization Report No.
Judy L. Shinn	L-13341
	10. Work Unit No.
9. Performing Organization Name and Address	506-51-23-01
NASA Langley Research Center Hampton, VA 23665	11. Contract or Grant No.
	13. Type of Report and Period Covered
12. Sponsoring Agency Name and Address	Technical Paper
National Aeronautics and Space Administration Washington, DC 20546	14. Sponsoring Agency Code

15. Supplementary Notes

16. Abstract

An experimental investigation of inviscid real-gas effects on the pressure distribution along the Space Shuttle Orbiter nose center line up to an angle of attack of 32° was performed in the Langley Expansion Tube in support of the Shuttle Entry Air Data System (SEADS), which is an instrumentation system for the Orbiter Experiment (OEX) Program. Free-stream velocities from 4.8 to 6.6 km/s were generated at hypersonic conditions with helium, air, and CO_2, resulting in normal-shock density ratios from 3.7 to 18.4. The experimental results for pressure distribution agreed closely with numerical results using the method of Moretti and Bleich (AIAA J., vol. 5, no. 9, 1967). Modified Newtonian theory deviates from both experiment and the numerical results as angle of attack increases or shock density ratio decreases. An evaluation of the use of modified Newtonian theory for predicting SEADS pressure distributions in actual flight conditions was made through comparison with numerical predictions.

17. Key Words (Suggested by Author(s))	18. Distribution Statement
Shuttle Entry Air Data System Inviscid real-gas effects Hypervelocity flow Space Shuttle Three-dimensional flow	Unclassified - Unlimited Subject Category 02

19. Security Classif. (of this report)	20. Security Classif. (of this page)	21. No. of Pages	22. Price*
Unclassified	Unclassified	26	$4.50

*For sale by the National Technical Information Service, Springfield, Virginia 22161

NASA-Langley, 1980